π−Conjugation Effect on the Aggregation−Induced Emission of Extended Viologens

Journal:	*New Journal of Chemistry*
Manuscript ID	NJ-ART-10-2020-005075.R2
Article Type:	Communication
Date Submitted by the Author:	23-Nov-2020
Complete List of Authors:	Tonga, Murat; University of Massachusetts Amherst, Chemistry

COMMUNICATION

π–Conjugation Effect on the Aggregation–Induced Emission of Extended Viologens

Received 00th January 20xx,
Accepted 00th January 20xx

DOI: 10.1039/x0xx00000x

Murat Tonga *[a, b]

This work focuses on the AIE properties of extended viologens (EVs), specifically the effect of π–conjugation by employing several aryl groups including phenyl, naphthyl, and anthryl. The DFT calculations show that these EVs with larger aryl groups adopt a twisted geometry due to steric hindrance between aryl and vinylene–pyridinium units, while the EV with phenyl ring adopted a planar one.

Recent decades have witnessed the evolution of luminescent materials which have been widely investigated in numerous areas such as electronics, optics, and biotechnology.[1] Most of the applications typically require strong emission in the solid–state. However, many traditional luminescent materials easily undergo an undesired aggregation–caused quenching (ACQ) due to the formation of unfavorable species such as excimers as a result of strong π–π interactions in the solid–state.[2] This causes huge limitations in practical applications. With the discovery of an opposite effect -- the aggregation–induced emission (AIE) -- which is an enhancement of emission in the aggregate/solid–state, a new route has emerged for the development of advanced functional material.[3] The AIE luminescent materials show a quenched or weak emission in solution state but emit strongly in the aggregate/solid–state. In general, the AIE molecules attain a twisted conformation which prevents the molecule to have a strong π–π stacking. Although the cause is still unknown, the mainly accepted mechanism is the restriction of intramolecular motions (RIM) which stems from structural planarization, *J*–aggregates, excited-state intramolecular proton transfer (ESIPT), twisted intramolecular charge transfer (TICT), and E/Z isomerization.[4] In the aggregate state, the RIM process blocks the excimer decay through the non–radiative pathways which cause the radiative channel to become the main deactivation pathway, thus leading to an intense emission.

Extended viologens, 1,1′–disubstituted–4,4′–bipyridinium organic salts, are a class of organic compounds made by the insertion of π–conjugated segments into the bipyridinium backbone. Their distinctive features including reversible redox, electrochromic and electron–withdrawing properties have found the versatility in various applications such as electrochromic devices,[5] molecular machines,[6] memory devices,[7] gas storage,[8] herbicide,[9] solar cells,[10] etc. Despite the remarkable accomplishments observed with extended viologens, the investigation of their AIE properties is still rare.[11] In an earlier article, we reported the synthesis and photophysical properties of some A–π–D–π–A type extended viologens.[12] In the present study, the AIE behaviors of the extended viologens shown in Scheme 1 were studied, particularly the effect of π–conjugation (i.e. phenyl, naphthyl, and anthryl). The AIE effects could benefit from the restriction of rotational and vibrational motions and *E*/*Z* isomerization of the vinylene–pyridinium units in the solid–state. Moreover, the vinylene units can cause a twisted geometry with the larger aryl backbones, which is beneficial to achieve an AIE property. Besides, electron–accepting property of the pyridinium units in the acceptor–donor–acceptor type design allowed accomplishing desirable AIE characteristics, especially the emission color (blue, green, and red emission) in a binary solvent system of acetonitrile and toluene.

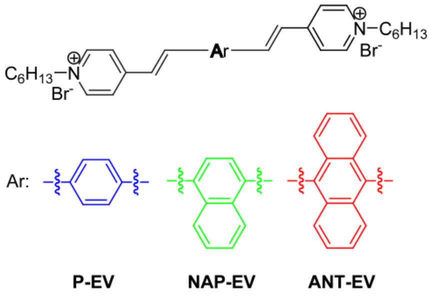

Scheme 1. Structures of the EV luminogens.

The synthesis and characterization of the EV luminogens, **P–EV** (phenylene–EV), **NAP–EV** (naphthalene–EV), and **ANT–EV** (anthracene–EV) were reported in our previous study.[12] Hexyl groups on the pyridinium termini were sufficient to dissolve these ionic luminogens in polar solvents such as methanol,

---

[a] Department of Chemistry, University of Massachusetts, Amherst, MA 01003, USA.
[b] Present Address: Polnox Corporation, 225 Stedman St # 23, Lowell, MA 01851, USA.
E-mail: murattonga@gmail.com; mtonga@Polnox.com

Electronic Supplementary Information (ESI) available: See DOI: 10.1039/x0xx00000x

acetonitrile (MeCN), and DMF. But, they are insoluble in nonpolar solvents like benzene, toluene, and diethyl ether.

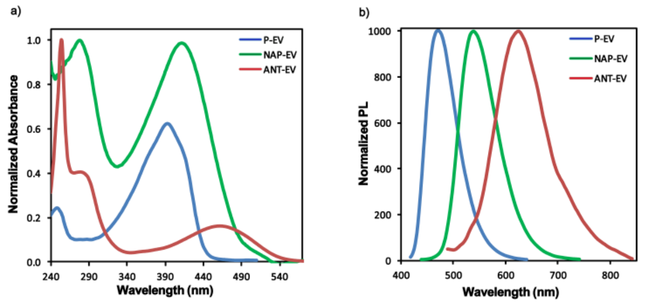

Figure 1. Normalized absorption (a) and photoluminescence spectra (b) of the EV luminogens in MeCN.

The UV–vis absorption and photoluminescence (PL) spectra of the EV luminogens in MeCN were demonstrated in Figure 1. and Table 1. The ICT process generally observed in the donor–acceptor systems are well–studied with the solution absorption spectroscopy to examine the excited state characteristics of these compounds, particularly π–conjugation extension. The similarities in their absorption bands imply that they are structural analogues (Figure 1a): the absorptions at ~ 240–340 nm (π–π* transition of the π–conjugated backbone) and ~ 340–560 nm (an ICT transition from donor to acceptor). The ICT peak maxima of the EV luminogens followed the increasing trend of π–conjugation: **P–EV** < **NAP–EV** < **ANT–EV**. Also, different ICT strength was noticed. For instance, NAP–EV has the highest ICT strength while **ANT–EV** has the lowest one. The weak ICT character of **ANT-EV** suggested its poor electronic communications due to the large distortion with the central anthryl core, which could be confirmed by computation modeling discussed below.[13] The maximum absorption peak of **NAP–EV** located at 411 nm was red–shifted by 18 nm relative to P–EV. The luminogen **ANT–EV** showed 69 nm redshift, due to the larger π–extension of anthryl compared to naphthyl. Figure 1b shows the normalized PL spectra of the EV luminogens. The PL spectra exhibited a similar trend as was observed for their absorbance spectra. Red–shifted PL spectra were observed with an increase in the π–conjugation: **P–EV** (79 nm), **NAP–EV** (128 nm), and **ANT–EV** (163 nm). The large Stokes shifts imply a large change in the dipole moment at the excited state.[14]

Table 1. Photophysical data of the EV luminogens.

	Abs$_{max}$ (π–π*) (nm)	Abs$_{max}$ (ICT) (nm)	PL$_{max}$ (nm)	Abs$_{onset}$ (nm)	Stokes Shift (nm)
P–EV	248	393	472	450	79
NAP–EV	278	411	539	537	128
ANT–EV	254	462	625	624	163

The AIE features of the EV luminogens were studied by precipitating the MeCN (5 μM) solution with the addition of different toluene fractions ($f_{toluene}$ = 10–90%). **P–EV** showed a moderate emission in the pure MeCN (Figure 2a). The PL intensity initially increased drastically at $f_{toluene}$ = 10% due to the change in solvent polarity. It is possible that **P–EV** molecules can form randomly packed amorphous aggregates which usually have weak π–π interactions, thereby boosting up the PL intensity.[15] However, the PL intensity starts to diminish with the added $f_{toluene}$ = 30–50% and it almost gave the intensity of the pure MeCN solution at $f_{toluene}$ = 50%. Upon further increasing $f_{toluene}$ to 70–90% nearly caused a complete quenching in the emission, which could be ascribed to the formation of crystalline aggregates. At higher $f_{toluene}$, the crystalline aggregates of **P–EV** built in a well–ordered fashion can have strong π–π stacking which can cause the formation of detrimental species, thus decreasing the emission intensity. The overall PL intensity is determined by the collective effects of the two kinds of aggregates. However, it is difficult to control the formation of aggregates in high toluene content since toluene is not a suitable solvent for these organic salt molecules. Thus, the PL intensity might demonstrate irregularities in high toluene content. Mie or the light scattering effect obstructs the accurate determination of quantum yields.[16] Therefore, the change in the PL peak intensity (I/I_0 ratio, where I is the peak intensity in the MeCN–Toluene mixture and I_0 is in the pure MeCN) with added $f_{toluene}$ was calculated to evaluate the AIE effect. At $f_{toluene}$ = 10%, the emission intensity was enhanced more than 3–times compared to the pure MeCN solution and about 20–times compared to the aggregate state formed at $f_{toluene}$ = 90%, which is the most quenched state. Then, it demonstrated a downward trend by acquiring a 2–times enhancement in the intensity until $f_{toluene}$ reaches 50%, which nearly showed the same intensity with the pure MeCN solution. It was also noticed that the PL peak maxima of **P–EV** aggregates remained almost steady when $f_{toluene}$ = 10–50% and then they showed 22–32 nm redshifts beyond the $f_{toluene}$ > 50% (Figure 2b). Under illumination with a 365 nm UV lamp, a blue emission located at 475 nm was observed for the aggregates formed at the $f_{toluene}$ = 10–50% (Figure 2b–inset). Hence, it can be inferred that **P–EV** is AIE–active.

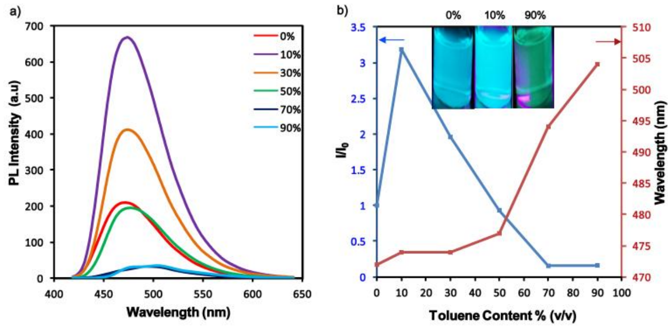

Figure 2. AIE results of **P–EV** in MeCN–Toluene solvent systems.

Similarly, the AIE properties of the EV luminogen **NAP–EV** were also attempted in the MeCN–Toluene solvent system (Figure 3a). The AIE effect arises from the RIM of the naphthyl backbone and the vinylene–pyridinium units. The PL intensity decreased gradually with the added $f_{toluene}$ = 30%, which could be explained by the formation of crystalline aggregates. Then, it intensifies noticeably when the $f_{toluene}$ reaches 50%, presumably by forming amorphous aggregates. Further increasing the $f_{toluene}$ completely quenched the emission at $f_{toluene}$ = 90%. Many AIE designs also had a similar issue, but the reason is not clear yet. It is speculated that these aggregates could be produced by the reorganization of the aggregates into the well–organized structures at higher fractions of a precipitating solvent.[17] At $f_{toluene}$ = 50%, the PL intensity rose by

~1.2–times compared to the pure MeCN solution and ~45–times compared to the aggregate state formed with added f_{toluene} = 90%, which is the most quenched phase (Figure 3b). A steady trend in the position of the emission maxima was noted until f_{toluene} reaches 70% and then it was red–shifted by 93 nm at ft_{oluene} = 90%. Thus, AIE–active **NAP–EV** showed a green emission (λ_{PL} = 543 nm) at the f_{toluene} = 50%.

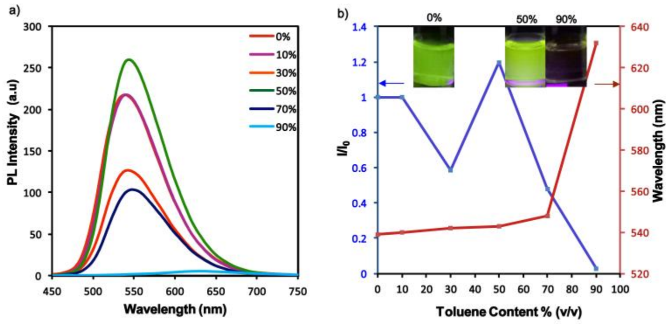

Figure 3. AIE results of **NAP–EV** in MeCN–Toluene solvent systems.

The EV luminogen **ANT–EV** in the pure MeCN solution had a weak emission compared to **P–EV** and **NAP–EV**. Figure 4a demonstrates that the PL intensity remained relatively constant when the f_{toluene} = 10–70%. Then, it increased dramatically at f_{toluene} = 90%. At higher toluene fractions, the twisted nature of the anthryl core and the vinylene groups restricts π–π interactions, which leads to an intense emission.[18] The PL peak intensity (I/I_0 ratio) at f_{toluene} = 90% was determined as ~4.5–times higher than that of pure MeCN solution (Figure 4b). The improvement in the emission intensity was also accompanied by some shifts in the PL peak as f_{toluene} varies. Initially, it was quite stable when $f_{\text{toluene}} \leq 50\%$, then it red–shifted by 8 nm for f_{toluene} = 70%, and finally it blue–shifted by ~20 nm at f_{toluene} = 90%. It was noteworthy that accomplishing an AIE effect with a blue shift in the emission is an atypical event and it is called as aggregation–induced blue–shifted emission (AIBSE). It has been observed in some 9,10–substituted anthracene molecules.[19] The cause is still unknown; however, it might be the change in the conformation during the aggregation process suppressing the formation of a charge transfer state.[20] The aggregates of **ANT–EV** generated with added f_{toluene} = 90% exhibited a red emission located at 606 nm as shown under illumination with a 365 nm UV lamp (Figure 4b–inset).

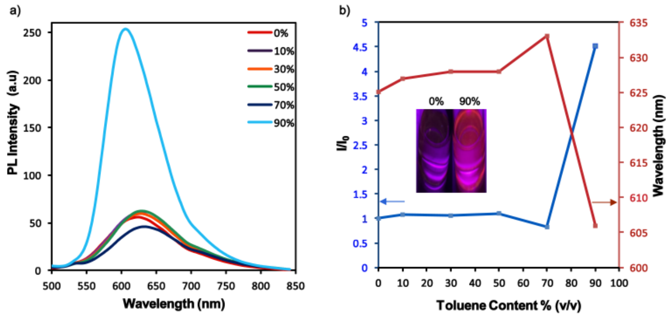

Figure 4. AIE results of **ANT–EV** in MeCN–Toluene solvent systems.

Color–tunable luminescent materials are advantageous for the advancement of optoelectronic devices, particularly for the generation of white light. These EV luminogens accomplished tunable emissions of blue (**P–EV**), green (**NAP–EV**), and red color (**ANT–EV**) at the aggregate states by simply altering the amount of nonpolar solvent toluene in the mixed solvent system. The CIE 1931 coordinates of the EV luminogens are shown in the chromaticity diagram in Figure S1. The white light emission is typically produced by mixing two or more complementary colors (blue and green or red, green, and blue) that span the full visible region (400–700 nm).[21] Interestingly, the resulting emission maxima of the aggregate states of the EV luminogens cover the required RGB spectrum (Figure S1). Therefore, these EV luminogens could be good candidates to produce white light. Additional experiments would be required to investigate this further.

The optimized geometries could be useful to gain insight into the relationship between the structures and AIE features of the EV luminogens in the absence of the crystal structures. To investigate this, density functional theory (DFT) was studied using the Spartan 04 program at the B3LYP/6–311G* level. Table S1 presents their dihedral angles and the frontier orbital energy levels. The dihedral angles at specific sites can assist to understand the conformation of the EV luminogens. Therefore, the dihedral angles α, β, and γ were thoroughly investigated; where α is described as the angle between the central aromatic groups (phenyl, naphthyl, and anthryl) and the vinylene unit, β is the angle between the pyridinium unit and the vinylene unit, and γ is the angle between pyridinium unit and the central aromatic groups.

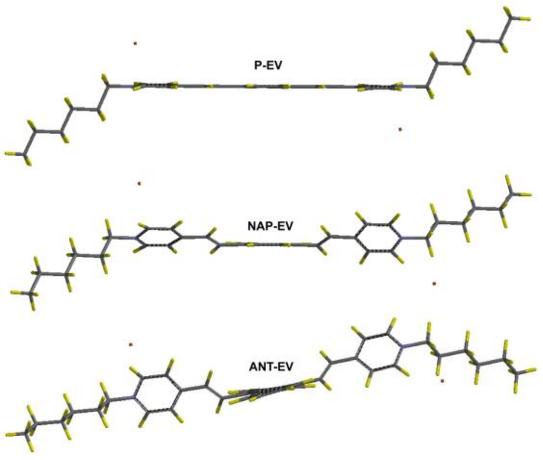

Figure 5. The optimized geometries of the EV luminogens. The small red dots represent the bromide ions.

As shown in Figure 5, the luminogens **NAP–EV** and **ANT–EV** adopted a twisted geometry where the vinylene and pyridinium units are forced out of the central aryl core due to steric hindrance. However, this steric hindrance is almost canceled out in the luminogen **P–EV** by adopting a highly planar geometry with the dihedral angles of α = 1.3°, β = 3.4°, γ = 4.7°. Although **P–EV** has a less distortion (or a quite planar) according to computation, it showed a stronger PL intensity than **NAP–EV** having a more twisted conformation. It may stem from the isomerization of double bond through E/Z conversion upon excitation, which could consume the excited state energy via non–radiative decay. However, this conversion process is hindered in the aggregate state, which causes an AIE effect.[22] The photoisomerization is most likely difficult for the luminogens **NAP–EV** and **ANT–EV** since they have large backbones. The dihedral angles were much higher for **NAP–EV** and **ANT–EV** which stems from a large distortion between central aryl core and the vinylene–pyridinium segments. The RIM in the solution phase gives rise to non–radiative pathways which quench the PL. However, in the aggregate state, the restriction of such torsional angles blocks non–radiative channels which yield an AIE characteristic with a strong emission. Moreover, the anion–π+ interactions in which π–conjugated backbone intrinsically containing positive charges and counter anions might also cause the AIE behavior. Due to the position of the anions to π systems, the anion–π+ interactions could hinder π–π stacking by acting as a separator between the molecules.[23] Particularly, the distances between bromide anions and the pyridinium cations presented in Table S1 show that this distance was larger for the π–extended luminogens **NAP–EV** and **ANT–EV** (in the range of 3.3–3.9 Å) compared to **P–EV** (3.3 Å). It is known that an emission quenching occurs when the π–π stacking distance is smaller than 3.5 Å.[24] Thus, the anion–π+ interactions might also allow yielding the AIE effect. Further experiment is required to probe this.

Conclusions

All in all, this contribution presents the AIE properties of the extended viologens by investigating the impact of π–conjugation. The AIE aspects resulted from not only the restraint of the twisted conformation formed due to the free rotations of the double bond, but also E/Z isomerization of the double bonds in the solid–state. As a result of electron–withdrawing aspect of the pyridinium units (with a typical ICT transition) and variable π–extension in the acceptor–donor–acceptor design, the diverse PL colors (RGB colors) were readily obtained in the MeCN–Toluene solvent systems. Therefore, this work could lead to developing new designs to attain efficient RGB and white color systems in optoelectronic applications.

Conflicts of interest

There are no conflicts to declare.

Notes and references

1 a) J. Guo, Z. Zhao and B. Z. Tang, *Adv. Opt. Mater.*, 2018, **6**, 1800264. b) X. Y. Zhang, K. Wang, M. Y. Liu, X.Q. Zhang, L. Tao, Y. W. Chen and Y. Wei, *Nanoscale*, 2015, **7**, 11486. c) Y. Chen, Y. Bai, Z. Han, W. He and Z. Guo, *Chem. Soc. Rev.*, 2015, **44**, 4517. d) C. Wang and Z. Li, *Mater. Chem. Front.*, 2017, **1**, 2174.

2 J. B. Birks, Photophysics of Aromatic Molecules, Wiley, London, 1970.

3 J. Luo, Z. Xie, J. W. Y. Lam, L. Cheng, H. Chen, C. Qiu, H. S. Kwok, X. Zhan, Y. Liu, D. Zhu and B. Z. Tang, *Chem. Commun.*, 2001, **18**, 1740.

4 J. Mei, Y. Hong, J. W. Y. Lam, A. Qin, Y. Tang and B. Z. Tang, *Adv. Mater.*, 2014, **26**, 5429.

5 a) A. Beneduci, S. Cospito, M. La Deda and G. Chidichimo, *Adv. Funct. Mater*. 2015, **25**, 1240. b) L. Veltri, V. Maltese, F. Auriemma, C. Santillo, S. Cospito, M. La Deda, G. Chidichimo, B. Gabriele, C. De Rosa and A. Beneduci, *Cryst. Growth Des*. 2016, **16**, 5646. c) A. N. Woodward, J. M. Kolesar, S. R. Hall, N. -A. Saleh, D. S. Jones and M. G. Walter, *J. Am. Chem. Soc.*, 2017, **139**, 8467. d) I. Pibiri, A. Beneduci, M. Carraro, V. Causin, G. Casella, G. A. Corrente, G. Chidichimo, A. Pace, A. Riccobono and Giacomo Saielli, *J. Mater. Chem. C,* 2019, **7**, 7974. e) W. W. Porter, T. P. Vaid and A. L. Rheingold, *J. Am. Chem. Soc*., 2005, **127**, 16559.

6 a) S. Cantekin, A. J. Markvoort, J. A. A. W. Elemans, A. E. Rowan and R. J. M. Nolte, *J. Am. Chem. Soc*., 2015, **137**, 3915.

7 a) C. Zhang, Y. T. Tai, J. Shang, G. Liu, K. L. Wang, C. Hsu, X. Yi, X. Yang, W. Xue, H. Tan, S. Guo, L. Pan and R. W. Li, *J. Mater. Chem. C*, 2016, **4**, 3217. b) G. Liu, C. Wang, W. Zhang, L. Pan, C. Zhang, X. Yang, F. Fan, Y. Chen and R.-W. Li, *Adv. Electron. Mater*., 2016, **2**, 1500298.

8 a) O. Buyukcakir, S. -H. Je, D. S. Choi, S. N. Talapaneni, Y. Seo, Y. Jung, K. Polychronopoulou and A. Coskun, *Chem. Commun.*, 2016, **52**, 934.

9 a) S. J. Yuan, F. J. Xu, S. O. Pehkonen, Y. P. Ting, K. G. Neoh and E. T. Kang, *Biotechnol. Bioeng*., 2009, **103**, 268. b) Z. Shi, K. G. Neoh and E. T. Kang, *Langmuir*, 2004, **20**, 6847.

10 a) S. W. Boettcher, J. M. Spurgeon, M. C. Putnam, E. L. Warren, D. B. Turner-Evans, M. D. Kelzenberg, J. R. Maiolo, H. A. Atwater and N. S. Lewis, *Science*, 2010, **327**, 185.

11 a) S. K. Samantaa and S. Bhattacharya, *J. Mater. Chem*., 2012, **22**, 25277. b) J. Sun, Y. Lu, L. Wang, D. Cheng, Y. Sun and X. Zeng, *Polym. Chem*., 2013, **4**, 4045. c) M. Olesińska, G. Wu, S. Gómez-Coca, D. Antón-García, I. Szabó, E. Rosta and O. A. Scherman. *Chem. Sci*., 2019, **10**, 8806. d) F, Qiao, Z. Yuan, Z. Lian, C. -Y. Yan, S. Zhuo, Z. -Y. Zhou and L. -B. Xing, *Dyes Pigments*, 2017, **146**, 392-397.

12 M. Tonga and P. M. Lahti, *Synthetic Met*., 2019, **254**, 75.

13 J. Zhang, J. Chen, B. Xu, L. Wang, S. Ma, Y. Dong, B. Li, L. Ye and W. Tian, *Chem. Commun*., 2013, **49**, 3878.

14 S. S. M. Fernandes, M. C. R. Castro, A. I. Pereira, A. Mendes, C. Serpa, J. Pina, L. L. G. Justino, H. D. Burrows and M. M. M. Raposo, *ACS Omega*, 2017, **7**, 9268.

15 a) X. Q. Zhang, Z. G. Chi, B. J. Xu, C. J. Chen, X. Zhou, Y. Zhang, S. W. Liu and J. R. Xu, *J. Mater. Chem*., 2012, **22**, 18505. b) W. Huang, H. Zhou, B. Lib and J. Su, *RSC Advances*, 2013, **3**, 3038.

16 Y. Liu, X. T. Tao, F. Wang, J. Shi, J. Sun, W. Yu, Y. Ren, D. Zou and M. H. Jiang, *J. Phys. Chem. C*, 2007, **111**, 6544.

17 Y. N. Hong, J. W. Y. Lam and B. Z. Tang, *Chem. Commun*., 2009, **29**, 4332.

18 B. Xu, J. T. He, Y. J. Dong, F. P. Chen, W. L. Yu and W. J. Tian, *Chem. Commun*., 2011, **47**, 6602.

19 a) J. Huang, N. Sun, P. Chen, R. Tang, Q. Li, D. Ma and Z. Li, *Chem. Commun*., 2014, **50**, 2136. b) L. Bu, M. Sun, D. Zhang, W. Liu, Y. Wang, M. Zheng, S. Xue and W. Yang, *J. Mater. Chem. C*, 2013, **1**, 2028.

20 S. Banerjee, A. K. Both and M. Sarkar. *ACS Omega*., 2018, **3(11)**, 15709.

21 a) M. Chen, Y. Zhao, L. Yan, S. Yang, Y. Zhu, I. Murtaza, G. He, H. Meng and W. Huang, *Angew. Chem., Int. Ed.*, 2016, **56**, 722. b) A. Krishna, E. Varathan, P. Sreedevi, V. Subramanian, V. Karunakaran and R. L. Varma, *Dyes Pigments* 2018, **159**, 77.

22 J.-S. Ni, H. Liu, J. Liu, M. Jiang, Z. Zhao, Y. Chen, R.T.K. Kwok, J. W. Y. Lam, Q. Peng and B.Z. Tang, *Mater. Chem. Front.*, 2018, **2**, 1498.

23 a) J. Wang, X. Gu, P. Zhang, X. Huang, X. Zheng, M. Chen, H. Feng, R. T. K. Kwok, J. W. Y. Lam and B. Z. Tang, *J. Am. Chem. Soc*., 2017, **139**, 16974. b) K. Leduskrasts and E. Suna, *RSC Adv*., 2019, **9**, 460.

24 E. R. Jimenez and H. Rodríguez, *J. Mater. Sci*., 2020, **55**, 1366.

π–Conjugation Effect on the Aggregation–Induced Emission of Extended Viologens

Murat Tonga [a, b]

[a] *Department of Chemistry, University of Massachusetts, Amherst, MA 01003, USA*
[b] *Present Address: Polnox Corporation, 225 Stedman St Suite 23, Lowell, MA 01851, USA*
e-mail: murattonga@gmail.com; mtonga@Polnox.com
Phone: 1-413-545-2291, Fax: 1-413-545-4490

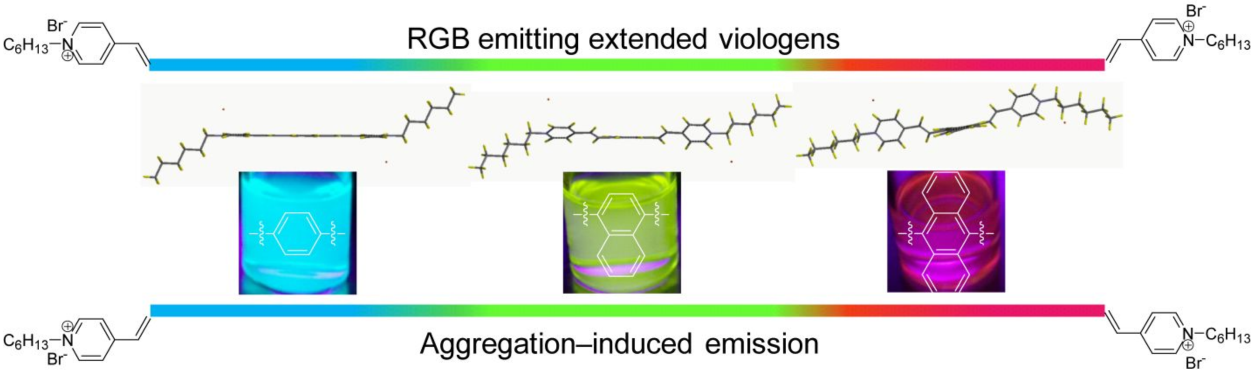

The aggregation–induced emission properties of extended viologens, particularly, -- the effect of π–conjugation -- were methodically studied.